© 2014. Published by The Company of Biologists Ltd | The Journal of Experimental Biology (2014) 217, 3133-3145 doi:10.1242/jeb.107383

RESEARCH ARTICLE

Opsin expression in *Limulus* eyes: a UV opsin is expressed in each eye type and co-expressed with a visible light-sensitive opsin in ventral larval eyes

Barbara-Anne Battelle[1,2,*], Karen E. Kempler[1,2], Alexandra Harrison[1,2], Donald R. Dugger[3] and Richard Payne[4]

ABSTRACT

The eyes of the horseshoe crab, *Limulus polyphemus*, are a model for studies of visual function and the visual systems of euarthropods. Much is known about the structure and function of *L. polyphemus* photoreceptors, much less about their photopigments. Three visible-light-sensitive *L. polyphemus* opsins were characterized previously (LpOps1, 2 and 5). Here we characterize a UV opsin (LpUVOps1) that is expressed in all three types of *L. polyphemus* eyes. It is expressed in most photoreceptors in median ocelli, the only *L. polyphemus* eyes in which UV sensitivity was previously detected, and in the dendrite of eccentric cells in lateral compound eyes. Therefore, eccentric cells, previously thought to be non-photosensitive second-order neurons, may actually be UV-sensitive photoreceptors. LpUVOps1 is also expressed in small photoreceptors in *L. polyphemus* ventral larval eyes, and intracellular recordings from these photoreceptors confirm that LpUVOps1 is an active, UV-sensitive photopigment. These photoreceptors also express LpOps5, which we demonstrate is an active, long-wavelength-sensitive photopigment. Thus small photoreceptors in ventral larval eyes, and probably those of the other larval eyes, have dual sensitivity to UV and visible light. Interestingly, the spectral tuning of small ventral photoreceptors may change day to night, because the level of LpOps5 in their rhabdoms is lower during the day than during the night, whereas LpUVOps1 levels show no diurnal change. These and previous findings show that opsin co-expression and the differential regulation of co-expressed opsins in rhabdoms is a common feature of *L. polyphemus* photoreceptors.

KEY WORDS: *Limulus* photoreceptors, UV opsin, UV sensitivity, Opsin co-expression, Diurnal rhythms

INTRODUCTION

The visual system of the American horseshoe crab, *Limulus polyphemus* (Linnaeus 1758), is a classic preparation for studies of phototransduction, light adaptation, retinal integration and circadian rhythms in retinal function. *Limulus polyphemus*, a xiphosauran chelicerate, occupies one of the most basal branches of the arthropod lineage (Regier et al., 2010), and so also may provide insight into the structure and function of the visual system of euarthropods. *Limulus polyphemus* has three types of eyes: a pair of median ocelli (ME), a pair of lateral compound eyes (LE) and three pairs of rudimentary or larval eyes – lateral, median (also called endoparietal) and ventral. The structure and function of *L. polyphemus* photoreceptors have been extensively studied, but not their photopigments, which consist of a chromophore derived from vitamin A bound to the protein opsin (Wald and Hubbard, 1950). The amino acid sequence of opsin primarily determines the spectral sensitivity of the photopigment and influences the dynamics of the photoresponse (Yokoyama, 2000).

In this study we examine opsin expression in each *L. polyphemus* eye type; therefore, the retinas and photoreceptors in each are introduced here. The locations of the eyes are shown in Fig. 1A. ME retinas (Fig. 1B) consist of loosely organized clusters of five to 11 photoreceptors below a single lens. Approximately 70% of ME photoreceptors are sensitive to UV light and 30% to visible light (Nolte and Brown, 1970). Each photoreceptor cluster is associated with one or two secondary visual cells called arhabdomeric cells (Jones et al., 1971; Fahrenbach and Griffin, 1975) that are electrically coupled to photoreceptors and generate action potentials when photoreceptors depolarize (Nolte and Brown, 1972). Both photoreceptors and arhabdomeral cells project to the brain, but because only graded, slow depolarizations have been recorded from photoreceptor axons (Behrens and Fahy, 1981), arhabdomeric cells are thought responsible for transmitting visual information to the brain.

LE retinas in adult animals consist of over 1000 well-organized ommatidia, each located below a conical lens (Fig. 1C). Each ommatidium contains five to 12 photoreceptors or retinular cells that in cross-section appear like the sections of an orange clustered around the dendrite of one to three secondary visual cells called eccentric cells. Eccentric cells are thought to be functionally equivalent to arhabdomeric cells in MEs (Waterman and Wiersma, 1954). Collaterals of eccentric cell axons also synapse with one another below the ommatidia in a plexus that is the anatomical substrate for lateral inhibition (Hartline et al., 1956; Fahrenbach, 1985). *Limulus polyphemus* is the only extant chelicerate with compound eyes.

Lateral, median and ventral larval eyes appear in the embryo before the more complex LEs and MEs (Harzsch et al., 2006). They are thought to provide photic input to embryos and newly hatched larvae, and they persist in the adult. Of the three pair of larval eyes, ventral eyes (VEs) are the best characterized. In adult animals, they consist of a pair of optic nerves that extend anteriorly from the brain and end beneath a specialized ventral organ on the ventral cuticle. Photoreceptor cell bodies cluster in an end organ (EO) at the distal end of each VE nerve and at its proximal end near the brain. They are also scattered along the length of the nerve (Fig. 1D) (Clark et al., 1969). In larvae and juvenile animals, VE nerves are not yet extended, so in young animals all VE photoreceptors cluster near the brain, and the ventral organ is located over the anterior brain.

[1]Whitney Laboratory for Marine Bioscience, University of Florida, St Augustine, FL 32080, USA. [2]Departments of Neuroscience and Biology, University of Florida, Gainesville, FL 32611, USA. [3]Department of Ophthalmology, University of Florida, Gainesville, FL 32610, USA. [4]Department of Biology, University of Maryland, College Park, MD 20742, USA.

*Author for correspondence (Battelle@whitney.ufl.edu)

Received 29 April 2014; Accepted 5 June 2014

The Journal of Experimental Biology (2014) doi:10.1242/jeb.107383

List of abbreviations

CNS	central nervous system
EO	end organ
ir	immunoreactive, immunoreactivity
LE	lateral eye
Lp	*Limulus polyphemus*
ME	median eye
ND	neutral density
Ops	opsin
PFA	paraformaldehyde
PB	phosphate buffer
PBS	phosphate-buffered saline
RACE	rapid amplification of cDNA ends
SDS	sodium dodecyl sulfate
UV	ultraviolet
VE	ventral eye

Ventral eyes contain two types of photoreceptors: giant photoreceptors with cell bodies measuring approximately 150×75 µm and small photoreceptors that are approximately half the size of the giant cells (Fig. 1E) (Calman and Chamberlain, 1982; Herman, 1991a). Giant photoreceptors typically consist of two prominent lobes: a rhabdomeral lobe (R-lobe) and an arhabdomeral lobe (A-lobe). Their rhabdom, which is mostly external, appears as a cap around the R-lobe. Rhabdoms of small photoreceptors may be external, as in the giant photoreceptors, or appear internal, located within calycle extensions of the A-lobe. VE nerves are estimated to have an equal number of giant and small photoreceptors, with small photoreceptors mostly clustered in and near the EO (Herman, 1991a). However, our detailed understanding of the physiology of the photoresponse in *L. polyphemus* comes exclusively from studies of giant photoreceptors.

All *L. polyphemus* eyes contain visible light-sensitive photoreceptors with peak sensitivity at approximately 520 nm. In addition, MEs contain photoreceptors sensitive to UV light (Murray, 1966; Brown et al., 1967; Nolte and Brown, 1970; Lall, 1970). Three predicted visible light-sensitive opsins (Ops) have been characterized from *L. polyphemus* – LpOps1, LpOps2 and LpOps5 (Smith et al., 1993; Katti et al., 2010). LpOps1 and LpOps2 differ in their coding regions by only four amino acids and cannot be distinguished from one another with either *in situ* hybridization or immunocytochemical assays. We refer to them here collectively as LpOps1-2. When expressed in *Drosophila melanogaster*, LpOps1 shows peak sensitivity at 513 nm (Knox et al., 2003). LpOps2 probably has the same spectral sensitivity because none of the amino acid differences between LpOps1 and 2 occurs at sites thought to influence spectral tuning (Smith et al., 1993). LpOps5, in contrast, was predicted to have a different spectral sensitivity because LpOps5 and LpOps1-2 cluster to different opsin clades, and their amino acid sequences differ at sites predicted to influence the spectral tuning of opsins (Katti et al., 2010). LpOps1-2 and LpOps5 are co-expressed in LE retinular cells and giant VE photoreceptors, but they have not been detected in ME rhabdoms (Katti et al., 2010).

In the present study, we characterize a *L. polyphemus* UV opsin (LpUVOps1). Surprisingly, cDNA fragments encoding this opsin were initially obtained from a 454 analysis of transcripts from VEs where no sensitivity to UV light had been reported. This prompted us to examine the distribution of LpUVOps1 in each of the three types of *L. polyphemus* eyes with *in situ* hybridization and immunocytochemical assays, and to test for UV light sensitivity in VEs. We also asked whether LpUVOps1 is co-expressed with visible-light-sensitive opsins, and whether the level of LpUVOps1 in

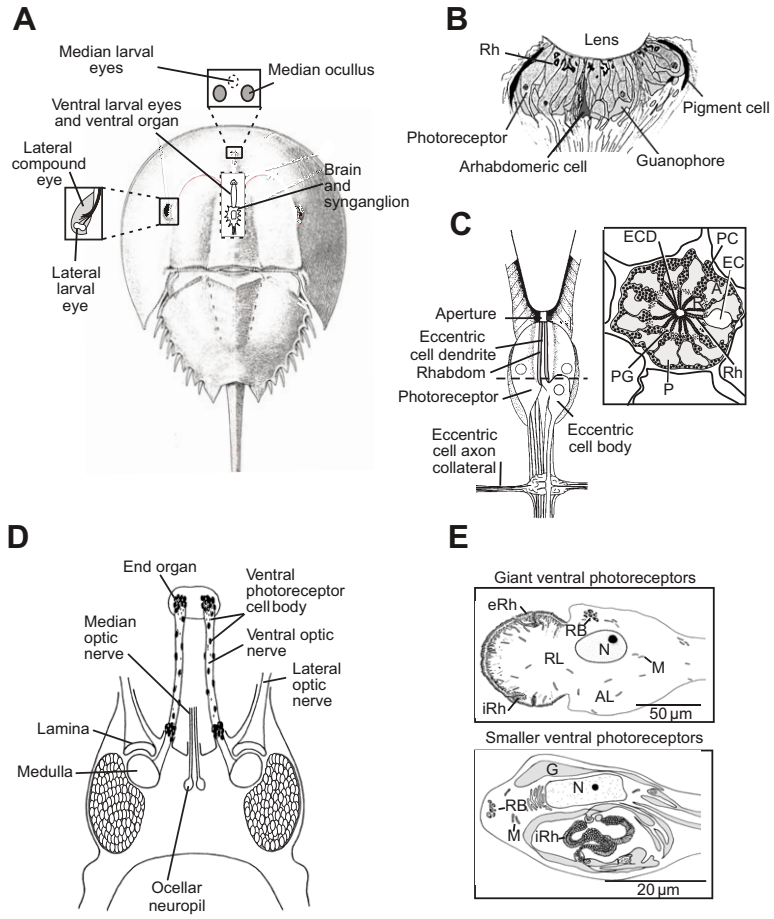

Fig. 1. The *Limulus polyphemus* visual system. (A) Schematic of a dorsal view of *L. polyphemus* showing the positions of its eyes. Box on the left: enlargement of the lateral compound eye to show the location of the lateral larval eye. Box above: location of the median larval eyes (MEs) beneath the carapace between the two median ocelli. Cutaway in the center: locations of the brain, synganglion (circumesophageal ring) and ventral larval eyes, which end beneath the ventral organ. (B) Schematic of a longitudinal section through a median ocellus. Rhabdoms (Rh) of ME photoreceptors are located in a layer close to the lens (modified from Jones et al., 1971). (C) Left: schematic of a longitudinal section through a lateral eye ommatidium. Right: schematic of a cross-section of a lateral eye ommatidium at the level of the dashed line on the left. (D) Schematic of a dorsal view of the brain and ventral optic nerves. The locations of the optic ganglia (lamina and medulla) and the ocellar neuropil are indicated. The dark ovals scattered along the optic nerves and clustered at the end organ and near the brain represent cell bodies of the giant and smaller ventral photoreceptors. (E) Diagrams of ventral photoreceptors. Top: giant ventral photoreceptors. Bottom: one of two types of smaller ventral photoreceptors. The type shown has an extensive internal rhabdom. A second type of smaller ventral photoreceptor has an external rhabdom and is organized much like the giant ventral photoreceptors. A, arhabdomeral segment; AL, arhabdomeral lobe; EC, eccentric cell body; ECD, eccentric cell dendrite; eRh, external rhabdom; G, glia; iRh, internal rhabdom; M, mitochondria; N, nucleus; P, photoreceptor cell; PC, pigment cell; PG, photoreceptor pigment granules; R, rhabdomeral segment; RL, rhabdomeral lobe; RB, residual bodies.

The Journal of Experimental Biology

The Journal of Experimental Biology (2014) doi:10.1242/jeb.107383

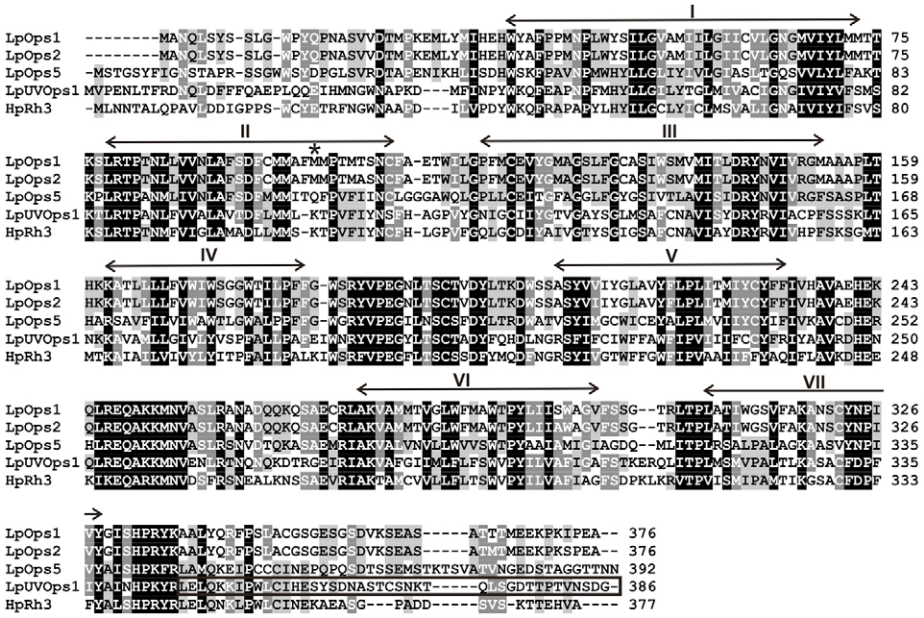

Fig. 2. Alignment of the predicted amino acid sequence of *L. polyphemus* UV opsin (LpUVOps1) with *L. polyphemus* opsins 1, 2 and 5 (LpOps1, LpOps2, LpOps5) and a presumptive UV-sensitive opsin from the jumping spider *Hasarium adansoni* (HaRh3). Positions of the transmembrane domains, indicted by the arrows above the sequences, are estimated from an alignment of bovine rhodopsin (Palczewski et al., 2000). Amino acids highlighted in black are identical or conserved in all four sequences; those in dark gray are identical or conserved in three; those in light gray are identical or conserved in two. The asterisk indicates the site equivalent to E^{90} in bovine rhodopsin that is responsible for determining UV sensitivity in rhabdomeral opsins. The C-terminal sequence of LpUVOps1 within the box was the antigen used to produce antibodies directed LpUVOps1.

rhabdoms changes with a diurnal rhythm as does LpOps1-2. This study also includes the first published electrophysiological recordings from small VE photoreceptors and spectral sensitivity curves for LpOps5.

RESULTS

A *L. polyphemus* UV opsin has been identified

The transcript identified in this study encodes a 44 kDa protein with features that identify it as a rhabdomeral opsin (Fig. 2): seven predicted transmembrane domains, a predicted glycosylation site in its N terminus (NQL^{13}) (http://www.cbs.dtu.dk/services/NetNGlyc), two conserved cysteine residues (C^{125}/C^{204}) that form a disulfide bond, a conserved lysine (K^{327}) in transmembrane helix VII that is the chromophore binding site, and a serine/threonine-rich C terminus. It also contains an amino acid triplet (HPR/K^{343}) near its C terminus, a characteristic of opsins that activate $G_{q/11}$ GTP binding proteins, and a string of eight amino acids in cytoplasmic loop three that is highly conserved among arthropod opsins (R^{253}–N^{260}) (Porter et al., 2007). We identify the protein as a UV-sensitive photopigment because its sequence has a lysine at the site equivalent to E^{90} in bovine rhodopsin, a characteristic of UV-sensitive rhabdomeral opsins (Salcedo et al., 2003). Furthermore, in a phylogenic analysis (Fig. 3), it clusters with high confidence among other arthropod UV-sensitive opsins. We call this opsin *L. polyphemus* UVopsin1 (LpUVOps1, accession number JN210564).

Distribution of LpUVOps1 transcripts

Using primers specific for the LpUVOps1 transcript and designed to amplify across an exon/intron boundary (6387567 F1 and 6189070 R2; supplementary material Table S1), we amplified an appropriately sized product from cDNA libraries of MEs and LEs (Smith et al., 1993) and an expressed sequence tag collection from VEs (Katti et al., 2010). This suggested that LpUVOps1 is expressed in all three eye types. Results of *in situ* hybridization assays were consistent with this suggestion (Fig. 4). On sections of MEs, LpUVOps1 antisense probe labeled cells in the photoreceptor layer. In whole mounts of VEs it labeled small photoreceptors clustered near the EO but not giant photoreceptors. On sections of LEs it labeled eccentric cell bodies and glia surrounding LE ommatidia, but not retinular cells. When ME sections and VE whole mounts were incubated with LpUVOps1 sense probe, no label was detected. LE sections incubated with sense probe showed no label over eccentric cell bodies, but glial labeling persisted; therefore, glial labeling is considered non-specific. These findings point to LpUVOps1's expression in ME photoreceptors, small VE photoreceptors and LE eccentric cells.

Distribution of LpUVOps1 protein

Antibody specificity

The specificity of a monoclonal antibody generated against the C terminus of LpUVOps1 (anti-LpUVOps1) (Fig. 2) was first tested on western blots of heterologously expressed C-terminal sequences of LpUVOps1, LpOps5 and LpOps1. Anti-LpUVOps1 immunostained the C terminus of LpUVOps1 but not LpOps5. Likewise, anti-LpOps5 immunostained the C terminus of LpOps5 but not LpUVOps1 (Fig. 5A). Similar assays (not shown) demonstrated that anti-LpUVOps1 does not immunostain LpOps1-2 and that anti-LpOps1-2 does not immunostain LpUVOps1.

Tissue distribution

Next, anti-LpUVOps1 was applied to western blots of membrane preparations from ME, LE and VE (Fig. 5B). On blots of ME membranes, anti-LpUVOps1 immunostained a single, major band with an apparent molecular mass of approximately 32 kDa. A band with the same apparent molecular mass was observed in membranes from VEs but not LEs. Higher molecular weight LpUVOps1-immunoreactive (ir) bands in the ME lane are probably opsin oligomers, which often form in sodium dodecyl sulfate (SDS) (Fliesler, 1993). The apparent molecular mass of LpUVOps1 observed on SDS gels is considerably lower than the mass determined from its amino acid sequence. This was not surprising as other opsins exhibit similar behavior (Battelle et al., 2001; Katti et al., 2010; Britt et al., 1993; Chou et al., 1996). When the blot was stripped and re-probed with anti-LpOps5, immunoreactive doublets at approximately 32 and 35 kDa were detected in membranes from VEs and LEs but not MEs. LpOps5 typically migrates as a doublet on SDS gels (Katti et al., 2010). The LpUVOps1-like-

The Journal of Experimental Biology (2014) doi:10.1242/jeb.107383

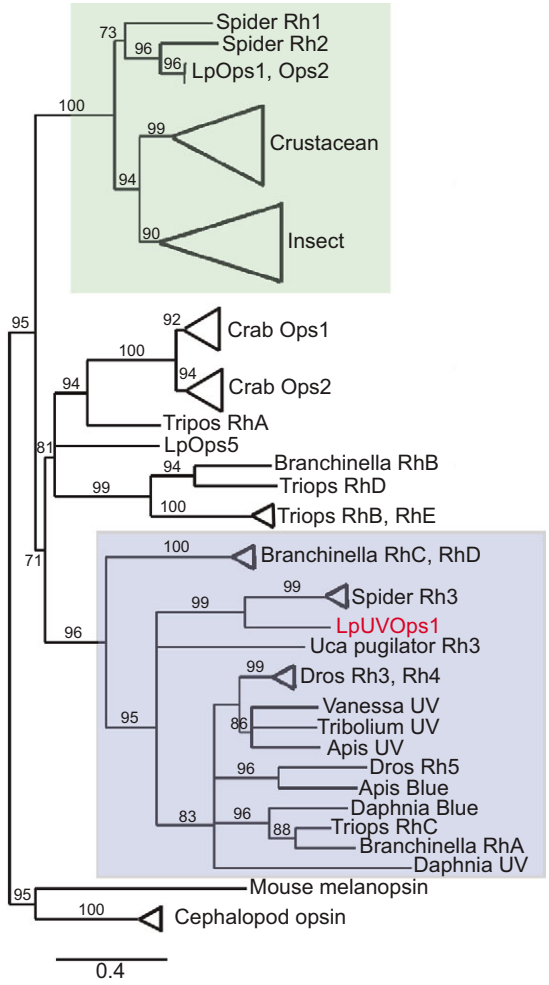

Fig. 3. Phylogenetic tree of arthropod opsins. Accession numbers for the sequences used to generate the tree are given in supplementary material Table S2. The tree was constructed using a maximum likelihood analysis of amino acid sequences. Numbers on the branches indicate approximate likelihood ratio test values for nodes supported by more than 70%. Major clades have been collapsed for clarity. Long-wavelength-sensitive opsins are highlighted in green; UV-short wavelength opsins are highlighted in blue. The *L. polyphemus* sequence of interest in this study (red) clusters most closely with spider Rh3 within the UV-short wavelength opsin clade.

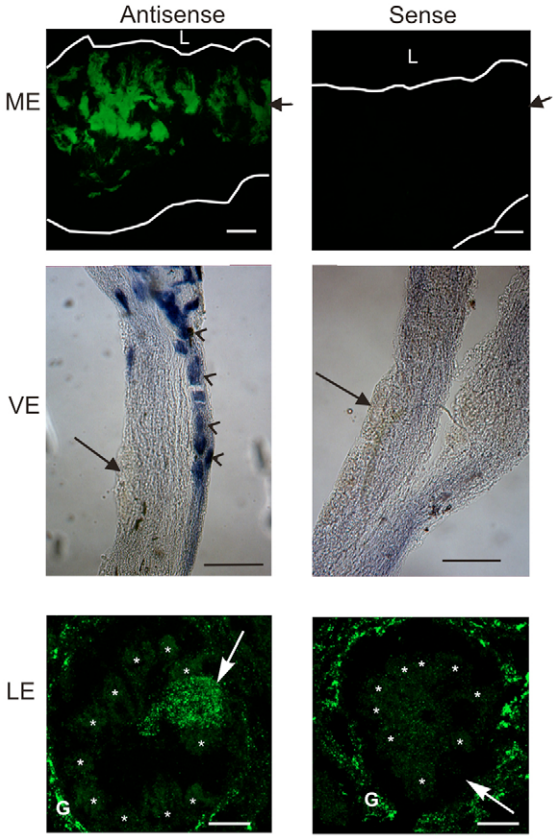

Fig. 4. *In situ* hybridizations showing the distribution of LpUVOps1 transcripts in median (ME), ventral (VE) and lateral eyes (LE). For MEs, oblique sections were incubated with sense and antisense probes that were visualized as fluorescein fluorescence using a confocal microscope. Images are maximum projections of 4–5 µm stacks. The tissue is outlined. L, position of the lens; arrows, position of the photoreceptor cell layer. Scale bars, 100 µm. For VEs, whole mounts were incubated with sense and antisense probes that were visualized using the NBT/BCIP reaction and viewed with a dissecting microscope. Small cells (arrowheads) labeled with the antisense but not the sense probe. Giant photoreceptors (arrows) did not label with either probe. Both images are from near the EO. Scale bars, 100 µm. For LEs, cross-sections incubated with antisense and sense probes were analyzed as described in A. Images are maximum projections of 13–15 µm stacks of images through individual ommatidia. The locations of retinular cell bodies (asterisks), eccentric cell bodies (arrows) and glia (G) are indicated. The antisense probe labeled eccentric cell bodies and glia surrounding ommatidia and but not retinular cells. The sense probe also labeled gial but did not label eccentric cell bodies. Scale bars, 50 µm.

immunoreactivity (ir) on western blots of ME and VE membranes was eliminated when the antibody was preincubated with antigen (Fig. 5C, UVOps1, Pre-Abs). These data indicate that anti-LpUVOps1 is specific for LpUVOps1 on western blots, and that the protein is present in ME and VE membranes.

Cellular distribution

The cellular distribution of LpUVOps1 was examined by applying anti-LpUVOps1 to sections of MEs, VEs and LEs together with an antibody directed against $G_{q/11}\alpha$ as a marker for rhabdoms. In MEs, anti-LpUVOps1 labeled most but not all rhabdoms (Fig. 6A,B). In VEs, it did not label giant photoreceptors, which can be recognized by the distinctive shape of their rhabdomeral lobes. Rather, it labeled what appear to be smaller photoreceptors (Fig. 6C). The specificity of LpUVOps1-ir on ME and VE tissues sections was confirmed with absorption controls (Fig. 6A,C, Pre-Abs). These results and results of the *in situ* hybridization assays (Fig. 4) indicate that LpUVOps1 is expressed in most ME photoreceptors and in small, but not giant, VE photoreceptors. Higher-power images of VE photoreceptors revealed LpUVOps1-ir in rhabdoms of both morphological types of small VE photoreceptors – those with an external rhabdomeral cap and those with an internal rhabdom (supplementary material Fig. S1) – but without an independent marker specific for small VE photoreceptors it cannot be determined whether all express LpUVOps1. The $G_{q/11}\alpha$-positive, LpUVOps1-negative rhabdoms seen in the merged image of Fig. 6C could originate from LpUVOps1-negative small cells or small sections through rhabdoms of giant photoreceptors.

Although LpUVOps1-ir was not detected on western blots of LE membranes, low-power images of cross-sections of LEs showed LpUVOps1-ir at the center of each ommatidium (Fig. 7A). This is the location of eccentric cell dendrites. LpUVOps1-ir in this region was eliminated by preincubating the antibody with antigen

The Journal of Experimental Biology (2014) doi:10.1242/jeb.107383

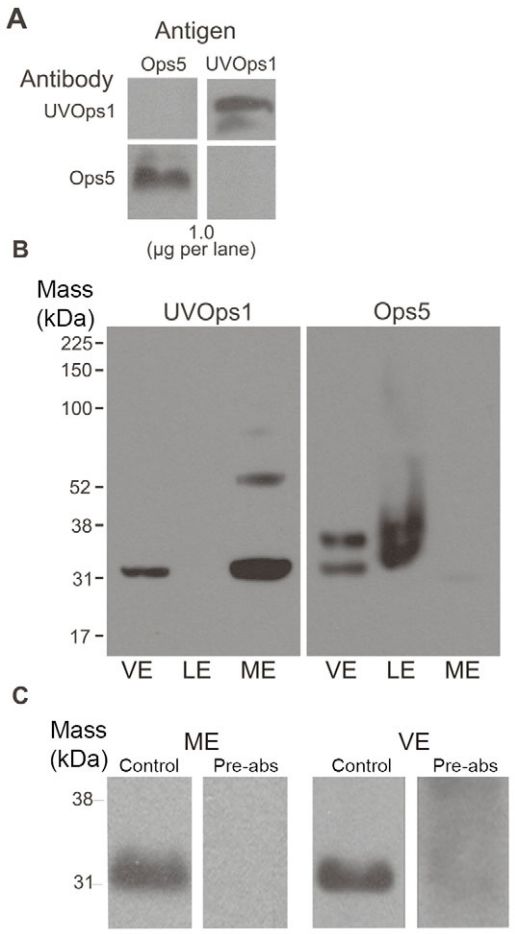

Fig. 5. LpUVOps1 is detected in membranes from VEs and MEs. (A) Chemiluminescent images of western blots of LpUVOps1 and LpOps5 antigens (1 µg per lane) probed with antibodies directed against these antigens. The blot was probed first with anti-LpUVOps1, stripped, and re-probed with anti-LpOps5. The antibody used is indicated on the left; the antigens are identified above the blots. Each primary antibody was diluted 1:1000; secondary antibodies were diluted 1:30,000. Each primary antibody labeled only the antigen against which it was generated. (B) Chemiluminescent images of western blots of membrane preparations from median eyes (ME), lateral eyes (LE) and ventral eyes (VE) probed with anti-LpUVOps1 and anti-LpOps5. Solubilized membranes from 2.5 VE nerves, 0.3 LEs and 0.5 MEs were loaded. Blots were immunostained for LpUVOps1 (1:50 dilution), stripped, then immunostained for LpOps5 (1:250 dilution). Anti-LpUVOps1 stained a single 32 kDa band from ME and VE membranes. No LpUVOps1-ir was detected in LE membranes. A doublet of LpOps5-ir at ~32 and 35 kDa was detected in membranes from LE and VE, but not ME. (C) Chemiluminescent images of western blots of ME and VE membranes probed with anti-LpUVOps1 (control, left lanes) and anti-LpUVOps1 that had been pre-absorbed with antigen (pre-abs, right lanes). Membranes were run on a single SDS gel separated by a lane of molecular mass markers. After proteins were transferred to nitrocellulose, the blot was cut so half the marker lane between the sample lanes was retained with each sample lane to allow the samples lanes to be aligned after immunostaining. Membranes from 1 ME were loaded on each lane and probed with either anti-LpUVOps1 or pre-absorbed anti-LpUVOps1 diluted 1:1000. Membranes from two VE nerves were loaded on each lane and probed with either anti LpUVOps1 or absorbed anti-LpUVOps1 diluted 1:50. Lanes probed with anti-LpUVOps1 each showed a clear band at approximately 32 kDa that was absent in lanes probed with pre-absorbed anti-LpUVOps1.

(Fig. 7B); thus immunostaining was specific. Higher-power images of oblique cross-sections through LE ommatidia revealed that LpUVOps1-ir is most intense where eccentric cell microvilli extend into the central collar of retinular cell microvilli (Lasansky, 1967; Fahrenbach, 1975) (Fig. 7C). The distribution of LpUVOps1-ir seen in longitudinal sections of ommatidia (Fig. 7D) is also consistent with the structure of eccentric cell dendrites that extend the entire length of ommatidia and taper toward the distal end (Lasansky, 1967; Fahrenbach, 1975). Longitudinal sections immunostained for LpUVOps1 and Ops5 also revealed a previously unidentified 'knot' of eccentric cell dendrite membranes approximately halfway along the length of ommatidia (Fig. 7D). These data, together with the results of *in situ* hybridization assays, lead us to conclude that LpUVOps1 is expressed in eccentric cell dendrites.

Is LpUVOps1 co-expressed with known visible-light-sensitive opsins?

In VEs, LpUVOps1 was not detected in giant VE photoreceptors (Fig. 8A), where LpOps1-2 and LpOps5 are co-expressed (Katti et al., 2010). However, in small VE photoreceptors LpUVOps1 was detected together with LpOps5 (Fig. 8B,C) but not LpOps1-2 (Fig. 8A). In MEs, co-expression of LpUVOps1with visible-light-sensitive opsin(s) cannot be determined because the visible-light-sensitive opsins expressed in MEs are not yet characterized. In LE eccentric cells, where LpUVOps1 is found, LpOps1-2 and LpOps5 transcripts have not been detected (Smith et al., 1993) (supplementary material Fig. S2).

In VEs, the level of LpOps5-ir in LpUVOps1-ir rhabdoms varied dramatically even among cells on the same VE nerve. In preparations dissected from daytime, light-adapted animals, LpOps5-ir was typically barely detected in LpUVOps1-ir cells located in or near the EO, whereas it was bright in LpUVOps1-ir rhabdoms of cells located more proximally along the nerve (Fig. 8B). However, in preparations from night-time, dark-adapted animals (Fig. 8C), LpOps5-ir was routinely detected in LpUVOps1-ir rhabdoms of EO cells as well as those located more proximally along the nerve. These observations suggest that a diurnal change in rhabdomeral levels of LpOps5 occurs in VE photoreceptors in the EO.

To test this, VEs were dissected within a block of tissue during the day in the light or during the night in the dark and fixed immediately. After the fixed tissue was rehydrated, VE nerves were dissected out, sectioned, immunostained for LpUVOps1 and LpOps5 and imaged with confocal microscopy. The average maximum intensity of LpOps5-ir in rhabdoms (rhabdomeral LpOps5) of giant photoreceptors in an EO was compared with that in giant cells located more proximal along the same VE nerve, as illustrated in supplementary material Fig. S3. At least four proximal and four EO photoreceptors were assayed from each of three night-time and three daytime animals. In night-time animals, rhabdomeral LpOps5 in EO and proximal photoreceptors was not significantly different (mean ± s.e.m. EO cells/proximal cells=1.25±0.38, P=0.6). However, in daytime animals, rhabdomeral LpOps5 was significantly lower in EO compared with proximal cells (mean ± s.e.m. EO cells/proximal cells=0.69±0.09, P<0.05). Thus, *in vivo*, light during the day reduced rhabdomeral LpOps5 in giant VE photoreceptors, and the reduction was greater in EO compared with proximal photoreceptors. Changes in LpOps5 in small VE photoreceptors could not be similarly quantified because too few were found isolated along the proximal VE nerve. However, consistent qualitative observations, such as those shown in Fig. 8B,C, indicate that rhabdomeral LpOps5 also decreases during the day in small VE photoreceptors in the EO. The different responses of EO

The Journal of Experimental Biology (2014) doi:10.1242/jeb.107383

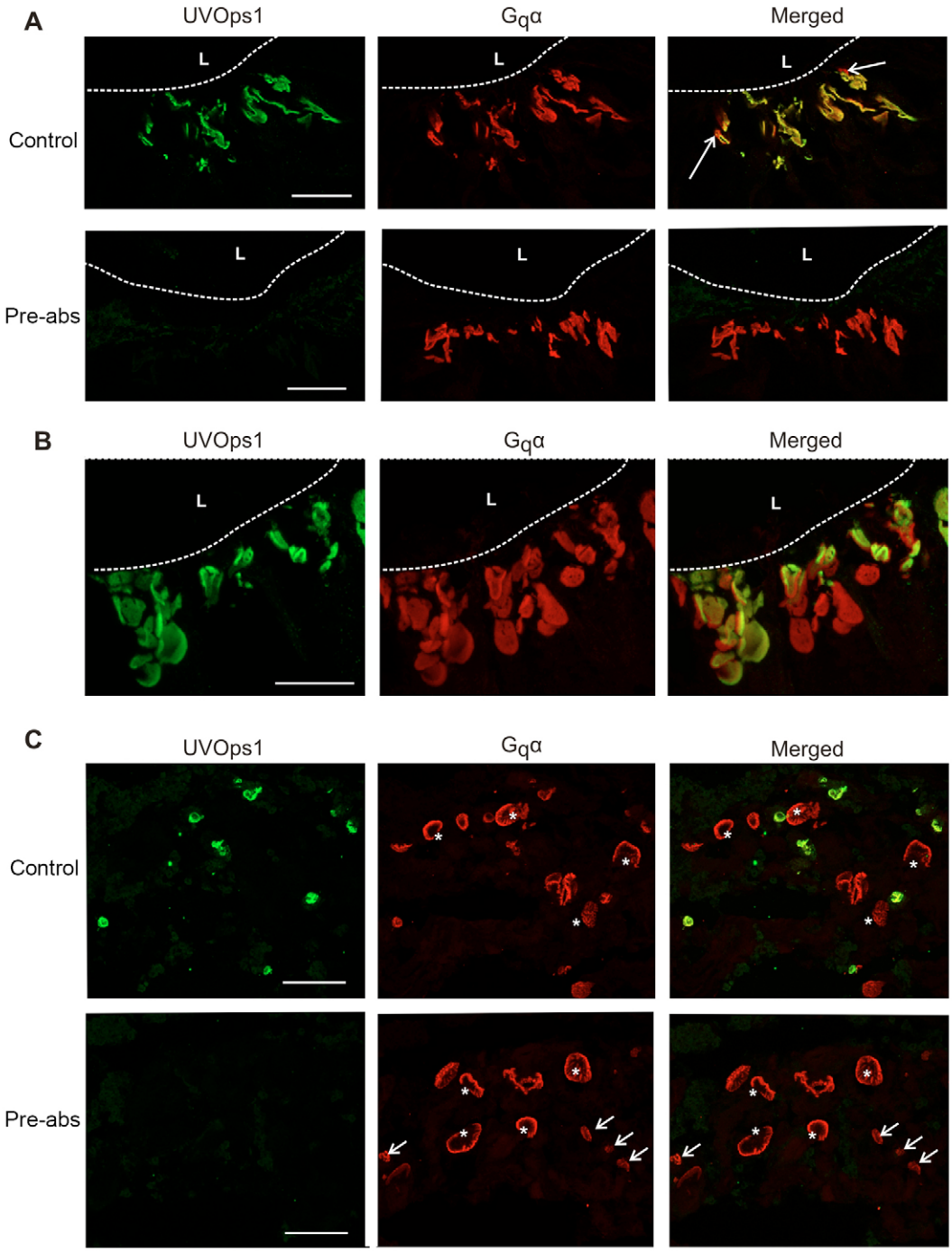

Fig. 6. LpUVOps1-ir is detected in rhabdoms of most ME photoreceptors and in small, but not giant, VE photoreceptors. (A) ME. Longitudinal sections were immunostained with anti-$G_{q/11}\alpha$ (1:1000 dilution, red) as a marker for rhabdoms and anti-LpUVOps1 (1:500 dilution, green; control) or anti-LpUVOps1 (1:500 dilution) that had been pre-absorbed with LpUVOps1 antigen (pre-abs). L, location of the lens; dashed line, base of the lens. In control sections, most rhabdoms were double labeled for $G_{q/11}\alpha$ and LpUVOps1, but some rhabdoms show no LpUVOps1-ir (arrows). Sections incubated with anti-LpUVOps1 that had been pre-incubated with antigen showed no LpUVops-ir. Images are maximum projections of 7 µm stacks. Scale bars, 50 µm. (B) Higher power image of LpUVOps1-positive and -negative ME rhabdoms that were immunostained as described for the upper panel in A. Images are maximum projections of 7 µm stacks. Scale bar, 25 µm. (C) VE end organ. Sections were immunostained with anti-$G_{q/11}\alpha$ (1:1000 dilution, red) as a marker for rhabdoms and anti-LpUVOps1 (1:500 dilution, green; control) or anti-LpUVOps1 (1:500 dilution) that had been pre-absorbed with antigen (pre-abs). On sections incubated with anti-LpUVOps1, LpUVOps1-ir was detected in some but not all cells. Cells with rhabdomeral profiles characteristic of giant ventral photoreceptors (asterisks) are not labeled. Sections incubated with pre-absorbed anti-LpUVOps1 showed no LpUVOps1-ir, although both giant (asterisks) and smaller (arrows) cells are in the section. Images are maximum projections of 32 µm (control) and 21 µm (pre-abs) stacks. Scale bars, 100 µm.

and proximal cells to daytime light *in vivo* are probably due to differences in the amount of light the cells were exposed to (see Discussion).

Distribution of UV light sensitivity

As described in the Introduction, photoreceptors with maximum sensitivity to UV light have been reported only in MEs. However,

The Journal of Experimental Biology (2014) doi:10.1242/jeb.107383

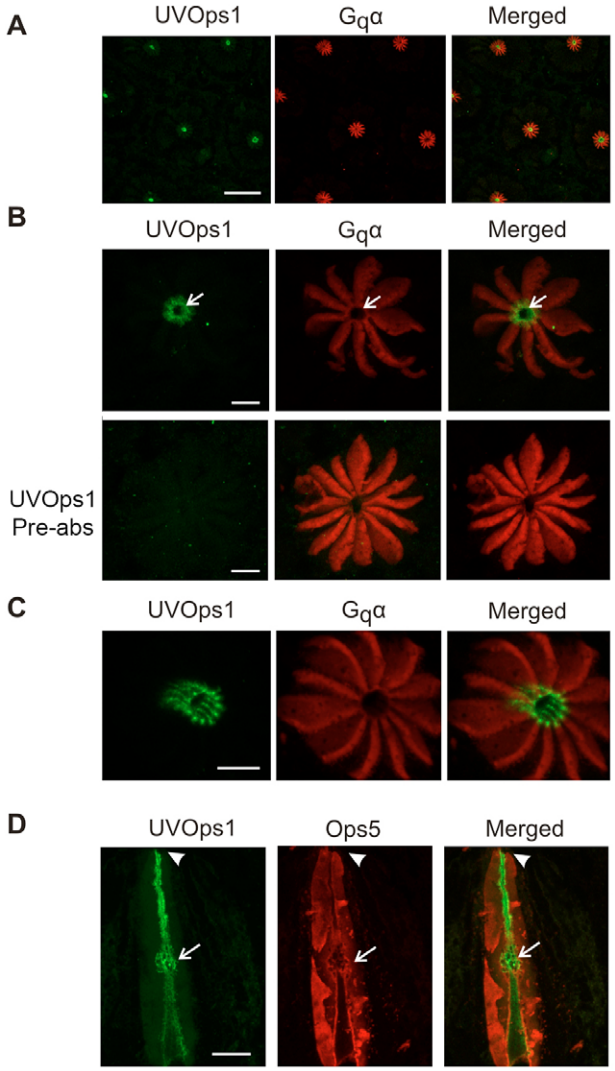

Fig. 7. LpUVOps1-ir is detected in dendrites of eccentric cells in LEs. (A) In LE cross-sections immunostained with anti-$G_{q/11}\alpha$ (1:1000 dilution, red) as a marker for rhabdoms and anti-LpUVOps1 (1:100 dilution, green), LpUVOps1-ir was seen at the center of each ommatidium in the location of the eccentric cell dendrite. Images are from a maximum projection of a 23 µm stack. Scale bar, 100 µm. (B) Cross-section of ommatidia immunostained with anti-$G_{q/11}\alpha$ (red) as in A, a 1:100 dilution of the anti-LpUVOps1 (upper panel) or a 1:100 dilution of pre-absorbed anti-LpUVOps1 (pre-abs). In sections incubated with anti-LpUVOps1, LpUVOps1-ir was consistently seen at the center of each ommatidium, the location of the eccentric cell dendrite (arrow). No LpUVOps1-ir was detected in sections immunostained with pre-absorbed anti-LpUVOps1. Images are maximum projections of 11 µm (upper panel) and 8 µm (pre-abs) stacks. Scale bars, 10 µm. (C) In a slightly oblique cross-section of an ommatidium immunostained as in A for $G_{q/11}\alpha$A (red) and LpUVOps1 (green), LpUVOps1-ir is most intense where microvilli of the eccentric cell dendrite extend into the central collar of retinular cell microvilli. Images are from a 5 µm stack. Scale bar, 10 µm. (D) The distribution of LpUVOps1-ir in a longitudinal section of LE ommatidia fixed during the day is consistent with its presence throughout the length of the eccentric cell dendrite. Sections were immunostained for LpUVOps1 (green) as in A and LpOps5 (1:500 dilution, red). Arrowheads, location of the base of the lens. LpUVOps1-ir is also detected in a knot of membranes located roughly half way down the length of the rhabdom (arrows). Images are maximum projections of 6–8 µm stacks. Scale bar, 25 µm.

because we detected LpUVOps1 in each type of *L. polyphemus* eye, the distribution of UV light sensitivity in *L. polyphemus* should be reinvestigated. In the present study, we focused on VEs.

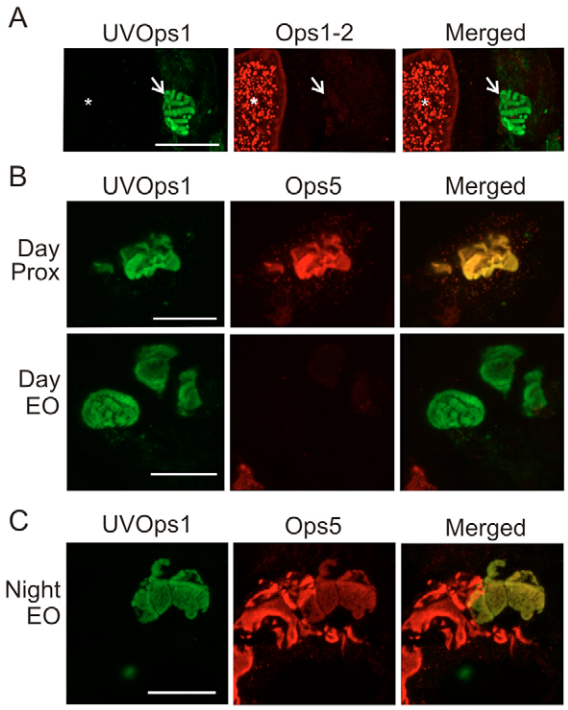

Fig. 8. LpUVOps1 is co-expressed with visible-light-sensitive LpOps5, but not LpOps1-2, in small VE photoreceptors. (A) LpUVOps1-ir is not detected with LpOps1-2-ir in giant VE photoreceptors (asterisks), and no LpOps1-2-ir is detected in cells expressing LpUVOps1 (arrows). Shown is a maximum projection of a 10 µm stack of optical images obtained from a VE section immunostained with anti-LpUVOps1 (1:100 dilution, green) and anti-LpOps1-2 (1:1000 dilution, red). VE nerves were fixed during the night in the dark. Scale bar, 25 µm. (B) In VE nerves fixed during the day in the light, LpUVOps1-ir is consistently detected together with LpOps5-ir in small VE photoreceptors, but the level of LpOps5-ir observed depends on the location of the photoreceptor on the VE nerve. VE sections were incubated with anti-LpUVOps1 (1:100 dilution, green) and anti-LpOps5 (1:100 dilution, red). Shown are maximum projections of 5–7 µm stacks of optical images through LpUVOps1-ir rhabdoms of two different cells on the same VE nerve. LpOps5-ir was bright in cells located proximal along the VE nerve (Prox) and barely detected in cells located in the EO. Scale bars, 20 µm. (C) In VE nerves fixed during the night in the dark, LpOps5-ir was clearly detected in LpUVOps1-ir rhabdoms of EO cells. Sections through and EO were immunostained as described in B. This maximum projection of a 7 µm stack of optical images shows a rhabdom of a small VE photoreceptor, which co-expresses LpUVOps1 and LpOps5, adjacent to rhabdoms of one or more giant cells expressing LpOps5 but not LpUVOps1. Scale bar, 20 µm.

Spectral sensitivities were first collected from isolated giant VE photoreceptors, which do not express LpUVOps1. Spectral sensitivity curves of four giant photoreceptors (Fig. 9A) showed a maximum at approximately 520 nm, with a secondary beta band of UV absorption. Average sensitivity in the beta band at 360 nm for the four cells was 0.85±0.27 $\log_{10}$ units less than that at the peak, consistent with previous results (Nolte and Brown, 1970). Thus, giant photoreceptors are approximately sevenfold less sensitive at 360 nm than at 520 nm. The spectral sensitivities could be reasonably well fit in the visible region with a template for rhodopsin absorption spectra proposed by Stavenga et al. (Stavenga et al., 1993), with the beta band peak absorbance set to be 0.85 $\log_{10}$ units less than the visible peak at 520 nm. In the UV region, the curves were much less well fit by the template, as previously noted generally for rhodopsin absorption spectra (Stavenga, 2010). Our results suggest that giant VE photoreceptors express rhodopsin(s) with a peak absorption of approximately 520 nm.

The Journal of Experimental Biology (2014) doi:10.1242/jeb.107383

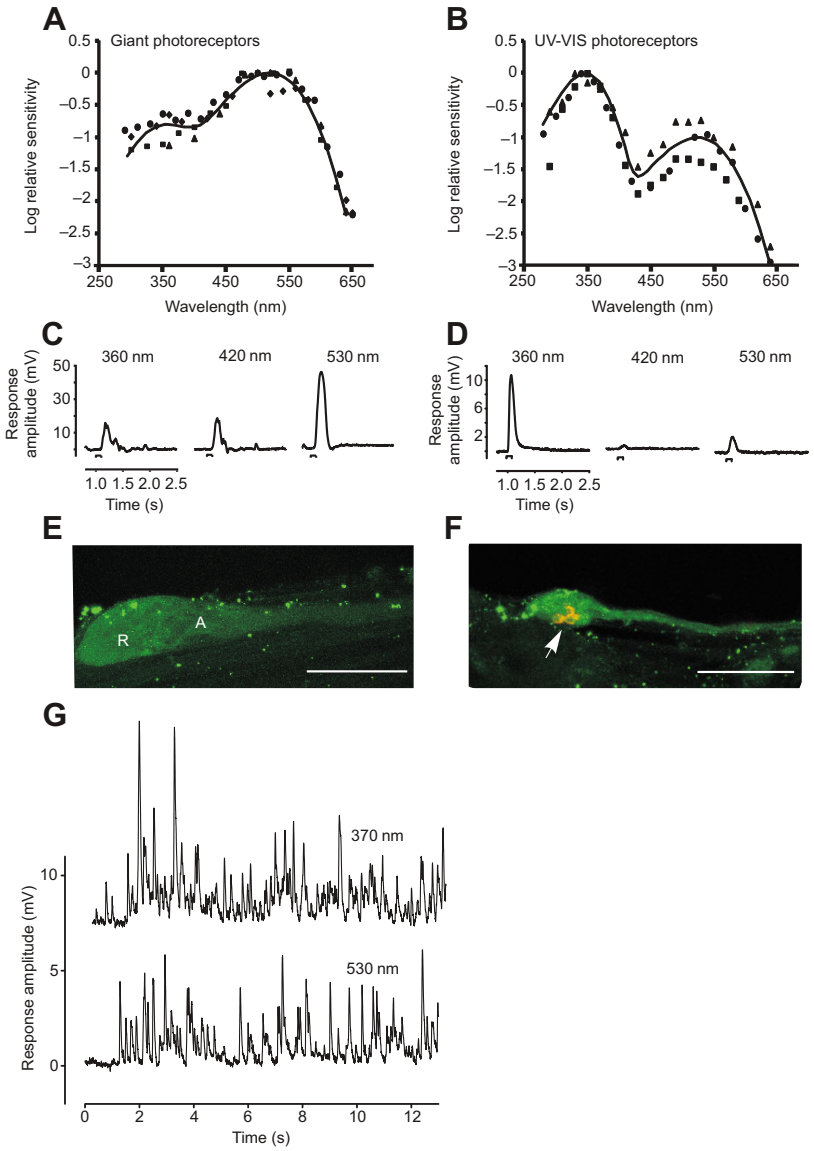

Fig. 9. Electrophysiological recordings for giant and small VE photoreceptors. (A,B) Spectral sensitivity of giant ventral photoreceptors (A) and UV-VIS-sensitive ventral photoreceptors (B). Spectral sensitivities were determined as described in the Materials and methods and expressed as the reciprocal of the intensity at each wavelength required to produce a criterion response. The peak of each spectral sensitivity curve was arbitrarily set to zero log units of attenuation. (C,D) Electrical responses of two different ventral photoreceptors to dim flashes attenuated by the same ND filter. C is the response of the photoreceptor shown in E; D is the response of the photoreceptor shown in F. Cells shown in E and F were filled with neurobiotin following stimulation and the entire root was fixed and immunostained for biocytin and LpUVOps1. (E) The cell has the size and shape typical for a giant ventral photoreceptor. The locations of the rhabdomeral (R) and arhabdomeral (A) lobes are indicated. (F) The cell has the size and shape typical for a smaller ventral photoreceptors and its rhabdom shows LpUVOps1-ir (arrow). Scale bars, 100 µm. (G) Photon shot noise recorded from UV-VIS ventral photoreceptors in response to a prolonged dim flash of light at 370 or 530 nm.

We also recorded responses of giant photoreceptors to dim flashes attenuated by the same neutral density (ND) filter at several wavelengths (Fig. 9C). As expected from the spectral sensitivity curves, the response to a 360 nm flash was comparable in amplitude to that of a 420 nm flash, although the lower lamp output in the UV and distortion by the cells' intensity–response function makes an exact comparison of response amplitude with spectral sensitivities impossible.

The immunocytochemical and *in situ* hybridization labeling for LpUVOps1 in VE (Figs 4, 6) indicates that cells expressing it are small and mostly scattered among clusters of photoreceptors near the EO. In view of the expected difficulties in locating and impaling these presumptive UV-sensitive cells, we needed a rapid screening strategy. We therefore searched close to the EO for impaled cells in which, in contrast to giant photoreceptors, the response to a 360 nm flash was greater than that to a 420 nm flash attenuated by the same ND filter (Fig. 9D). Spectral sensitivity curves measured from three cells that met this criterion (Fig. 9B) were very different from those of giant photoreceptors, showing a clear peak in the UV. Average sensitivity at 360 nm for the three cells was 0.89±0.36 $\log_{10}$ units greater than that at 520 nm. The variation in this ratio is consistent with that of the level of LpOps5-ir in LpUVOps1-ir rhabdoms of small VE photoreceptors. The spectral sensitivities of these cells could be reasonably fit with the sum of two templates for rhodopsin absorption spectra (Stavenga et al., 1993), with peak wavelengths at 348 and 525 nm, the latter being attenuated by 1 $\log_{10}$ unit. We call these UV-VIS cells.

To test directly whether the UV-VIS cells were small VE photoreceptors, photoreceptors showing spectral characteristics typical for UV-VIS cells (Fig. 9D) were filled with neurobiotin, and then the entire VE nerve was fixed, immunostained for biocytin and LpUVOps1, and viewed with a confocal microscope. Four such cells were filled on three separate VE nerves and all four had small cell bodies and expressed LpUVOps1-ir (Fig. 9F). As a control, four cells with spectral characteristics typical for giant photoreceptors (Fig. 9C) were also filled; these all showed typical giant photoreceptor morphology and no LpUVOps1-ir (Fig. 9E).

Our recordings also show that the time course of responses to UV and visible flashes in the UV-VIS cells were similar, and there was no discernible difference in the pattern of photon shot noise to dim flashes (Fig. 9G). These results are consistent with both opsins utilizing the same downstream transduction machinery. Our recordings suggest further that in UV-VIS cells located in or near the EO, the ratio of UV- to visible-light-sensitive opsins is

The Journal of Experimental Biology (2014) doi:10.1242/jeb.107383

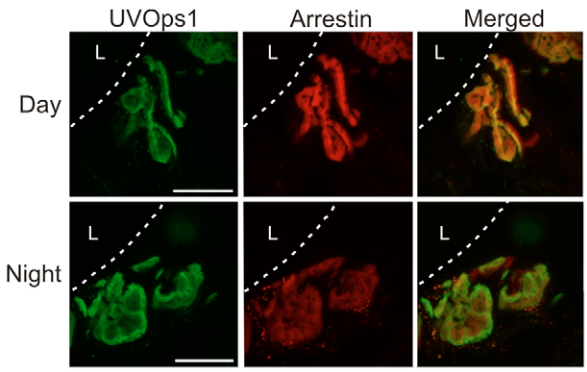

Fig. 10. In MEs, rhabdomeral LpUVOps1-ir does not change significantly day to night while rhabdomeral arrestin-ir is significantly higher during the day compared with during the night. MEs were from animals exposed to full spectrum sunlight during the day in an outdoor aquarium. Eyes were fixed in the light 30 min after peak illumination during the day or in the dark during the night 4 h after sunset. Shown are maximum projections of 4–6 µm stacks of optical images obtained from sections of MEs immunostained for LpUVOps1 (1:100 dilution, green) and arrestin (1:25 dilution, red). L, location of the lens. Dashed line, base of the lens. Scale bar, 20 µm.

approximately 10:1. However, this ratio must vary, because as was shown in Fig. 8, the level of LpOps5-ir in UV-VIS cells varies dramatically based on the cell's location along the VE nerve and time of day.

Is there a diurnal change in rhabdomeral levels of LpUVOps1?

A final question we asked was whether the level of LpUVOps1-ir in rhabdoms (rhabdomeral LpUVOps1) of ME and VE photoreceptors changes with a diurnal rhythm like LpOps1-2 in LE retinular cells and giant VE photoreceptors (Katti et al., 2010) and LpOps5 in VE photoreceptors in the EO (Fig. 8). To test this, we assayed rhabdomeral LpUVOps1-ir in MEs and VEs dissected from animals that had been exposed to full-spectrum sunlight in an outdoor aquarium. Eyes were fixed during the day in the light 30 min after peak illumination or during the night in the dark 4 h after sunset. VEs were fixed immediately within a block of tissue and subsequently dissected out. MEs from six daytime and six night-time animals were assayed, and average maximum intensities of LpUVOps1-ir in six to 10 separate rhabdomeres were assayed per animal. No significant diurnal change in mean (±s.e.m.) rhabdomeral LpUVOps1 was detected (day/night=107±9%, P=0.46; Fig. 10). As an independent test of whether the UV opsin-containing cells actually responded to light, rhabdomeral arrestin was measured in the same rhabdoms. Rhabdomeral arrestin increases in *L. polyphemus* photoreceptors in response to light (Battelle et al., 2013). In these rhabdoms, arrestin-ir was significantly higher during the day compared with during the night (mean ± s.e.m. day/night=220±24%, P>0.01; Fig. 10), confirming that the cells responded to light. Average rhabdomeral LpUVOps1 measured in six to 11 UV-VIS cells in ventral eye EOs of each of six daytime and six night-time animals exposed to full spectrum sunlight also showed no significant diurnal change (mean ± s.e.m. day/night=121±11%, P=0.097).

DISCUSSION

In this study we characterize a UV opsin from *L. polyphemus* (LpUVOps1) and show that it is expressed in each of the three types of *L. polyphemus* eyes. We show further that in small VE photoreceptors LpUVOps1 is co-expressed with LpOps5 but not LpOps1-2, and that these cells respond to both UV and visible light. Because LpOps5 is expressed in small VE photoreceptors in the absence of LpOps1-2 we were also able to extend our understanding of LpOps5. We show that it is an active photopigment with a spectral sensitivity similar to that of LpOps1-2, and that in VE photoreceptors located in EOs, rhabdomeral levels of LpOps5 change with a diurnal rhythm. By contrast, we found no significant diurnal change in rhabdomeral levels of LpUVOps1 in either VE or ME photoreceptors.

LpUVOps1 is expressed in most ME photoreceptors

Our immunocytochemical results (Fig. 6A,B) are consistent with previous studies showing that most ME photoreceptors are sensitive to UV light (Lall, 1970; Nolte and Brown, 1972) and that UV- and visible-light-sensitive ME photoreceptors are often closely associated with one another (Nolte and Brown, 1972). Prior electrophysiological studies further suggest that UV- and visible-light-sensitive opsins are not co-expressed in ME photoreceptors (Lall, 1970; Nolte and Brown, 1972). We could not address this question in the present study because the visible-light-sensitive *L. polyphemus* opsins characterized to date, LpOps1-2 and LpOps5, are not detected in ME rhabdoms (Katti et al., 2010).

LpUVOps1 is expressed in LE eccentric cells

This conclusion is based on our *in situ* and immunocytochemical results (Fig. 4B, Fig. 7). Our failure to detect LpUVOps1-ir on western blots of LE membranes (Fig. 5) is probably because eccentric cell membranes comprise only a small fraction of the total membrane in LEs, with most originating from the larger and more numerous retinular cells that express the visible-light-sensitive opsins LpOps1-2 and LpOps5 (Katti et al., 2010; Battelle et al., 2013).

Finding LpUVOps1 in LEs was surprising because prior spectral studies did not detect UV sensitivity in these eyes (Nolte and Brown, 1970; but see Wasserman, 1969). Recordings from retinular and eccentric cells also led to the conclusion that eccentric cells are not intrinsically photosensitive (Waterman and Wiersma, 1954). However, the apparent presence of LpUVOps1 in eccentric cell microvilli (Fig. 7C) leads us to speculate that eccentric cells are intrinsically photosensitive and contribute to the light response.

Eccentric cells are electrically coupled to retinular cells and depolarize when retinular cells are stimulated by visible light. But interestingly, the electrical junctions between retinular and eccentric cells are rectifying, such that depolarizing current flows from retinular to eccentric cells but not in the other direction (Smith and Baumann, 1969). Therefore, if eccentric cells depolarize in response to UV light, the current would not dissipate into retinular cells; rather, it could depolarize the eccentric cell sufficiently to produce action potentials or increase the likelihood that action potentials are produced in response to retinular cell depolarization. Thus, UV light may influence the output of LEs to the brain and, because collaterals of eccentric cell axons are the anatomical substrate for lateral inhibition, it may also influence the strength of lateral inhibition.

Our hypothesis that eccentric cells respond to light requires that all components for phototransduction are present in eccentric cell dendrites along with LpUVOps1. Components such as $G_{q/11}\alpha$ and arrestin are highly enriched in microvilli of the retinular cells with which eccentric cell dendrites are electrically coupled. Therefore, immunocytochemical studies at the light microscope level cannot resolve whether these components are also located at eccentric cell membranes. Future immunocytochemical studies at the electron

microscope level and electrophysiological studies are required to determine conclusively whether eccentric cells are UV photoreceptors.

LpUVOps1 expression in VEs reveals functional differences between the two structural classes of photoreceptors

Our results clearly show that the two structural classes of VE photoreceptors are functionally distinct. Giant VE photoreceptors express LpOps1-2 and LpOps5 and respond only to visible light, whereas small VE photoreceptors express LpUVOps1 and LpOps5 (Fig. 8) and respond to both UV and visible light (Fig. 10). Immunocytochemical assays revealed the same two classes of photoreceptors in lateral and median larval eyes (B.-A.B., unpublished data); thus *L. polyphemus* embryos and newly hatched larvae probably detect both visible and UV light with all of its larval eyes before the median and lateral eyes develop.

Light-dependent rhabdom shedding is also different in the two cell types. In giant VE photoreceptors, LpOps1-2-containing membrane is dramatically shed from rhabdoms in response to light (Katti et al., 2010), but as we show in the present study, light does not enhance LpUVOps1 rhabdom shedding in small VE photoreceptors or in LpUVOps1-expressing ME photoreceptors. LpOps5 is shed from rhabdoms in both giant (Katti et al., 2010) and small VE photoreceptors (Fig. 8) in a light-dependent manner, but LpOps5 shedding is modest compared with that of LpOps1-2. Our findings are consistent with previous observations showing that during dark–light transitions *in vitro*, rhabdoms of giant VE photoreceptors undergo dramatic structural changes associated with shedding while rhabdoms of small VE photoreceptors are relatively stable (Herman, 1991b).

Differential regulation of co-expressed opsins in rhabdoms

The three different photoreceptor types in *L. polyphemus* lateral and ventral eyes each express more than one opsin. LE retinular cells and giant VE photoreceptors co-express LpOps1-2 and LpOps5, and small VE photoreceptors co-express LpUVOps1 and LpOps5. Once thought rare, opsin co-expression has recently been described in insects (Ogawa et al., 2012; Hu et al., 2011; Hu et al., 2014), it may be common among crustaceans (Porter et al., 2013), and in *L. polyphemus*, a chelicerate, it appears to be the rule. A surprising finding in *L. polyphemus* is that relative rhabdomeral levels of co-expressed opsins in each of these three photoreceptor types change with a diurnal rhythm. Diurnal changes in relative levels of rhabdomeral LpOps1-2 and LpOps5 in LE retinular cells and giant VE photoreceptors were described previously (Katti et al., 2010; Battelle et al., 2013). The small VE photoreceptors described in the present study provide a third example. In EO photoreceptors of adult animals *in vivo*, rhabdomeral LpOps5 is lower during the day compared with during the night, whereas there is no diurnal change in rhabdomeral LpUVOps1.

No diurnal change in rhabdomeral LpOps5 was observed in proximal VE photoreceptors perhaps because, in adults, these photoreceptors are largely protected from light. The proximal VE nerve is well below the ventral cuticle surrounded by hepatopancreas and is protected from light by a layer of pigment cells underlying the cuticle. By contrast, EOs are directly attached to the cuticle at the VE organ, a specialized region of cuticle devoid of pigment and with a clear lens-like area located above each EO (Patten, 1894). Ventral photoreceptors in the EOs of adult animals can be exposed to light anytime the animal moves on its walking legs, swims inverted in open water or becomes inverted on beaches while spawning. In newly hatched trilobite larvae and young juveniles, a diurnal change in rhabdomeral LpOps5 probably occurs in all VE photoreceptors because these animals are largely transparent and also spend much time swimming upside down (B.-A.B., personal observation).

Light-dependent rhabdom shedding that decreases rhabdomeral opsin levels is not unique to *L. polyphemus*. In mosquitoes, for example, shedding dramatically reduces rhabdomeral opsin (Hu et al., 2012). *Limulus polyphemus* photoreceptors are the first in which a diurnal change in relative levels of co-expressed opsins in rhabdoms has been described (Katti et al., 2010; present study), but as rhabdomeral opsin levels are examined in more species under different conditions, more instances of this type of regulation will likely be observed.

The functional significance of diurnal changes in relative rhabdomeral levels of co-expressed opsins is not yet clear, and it may be different depending on the opsins that are co-expressed. It was speculated that LpOps1-2 and LpOps5 have different spectral sensitivities and that a diurnal change in their ratio in retinular cells and giant VE photoreceptors would change the spectral tuning of these cells (Katti et al., 2010). However, our current results show that in the visible range, peak sensitivity of small VE photoreceptors, which express LpOps5 and no LpOps1-2, is indistinguishable from that of giant VE photoreceptors (Fig. 10) and LE retinular cells (Graham and Hartline, 1935), both of which express LpOps1-2 and LpOps5 and in which LpOps1-2 is more abundant (Katti et al., 2010). This strongly suggests that the spectral sensitivities of LpOps1-2 and LpOps5 are similar and that a change in their ratio at rhabdoms will not change the cell's spectral sensitivity. Other aspects of photoreceptor function could be influenced, such as the dynamics of the photoresponse. However, another possibility is that additional, uncharacterized opsins are expressed in small VE photoreceptors and contribute to their spectral tuning in the visible range.

Regardless of whether additional visible-light-sensitive opsins are co-expressed with LpOps5 in small VE photoreceptors, a change in relative levels of LpUVOps1 and LpOps5 in their rhabdoms should influence these cells' spectral sensitivity. Our data suggest that these cells are relatively more sensitive to visible light during the night compared with during the day, whereas their sensitivity to UV light remains unchanged. As a consequence, the cell's sensitivity should shift toward the UV during the day. Because both LpUVOps1 and LpOps5 appear to couple to the same transduction cascade, wavelength information can be extracted from VEs, and probably other larval eyes, only by comparing responses of UV-VIS cells with other cells (i.e. the principle of univariance holds). To date, there is no evidence for color vision in *L. polyphemus*; therefore, the fundamental importance of UV opsin expression in each of the eyes may be to extend quantum capture into the UV range.

MATERIALS AND METHODS

Animals

Adult animals were collected from the Indian River near Melbourne, FL, USA. Those used for electrophysiological recordings were maintained on a 12 h:12 h light:dark cycle in aquaria with recirculating filtered artificial seawater (Instant Ocean, Aquarium Systems, Inc., Mentor, OH, USA) at a temperature of 15°C. All others were housed in natural, continuously flowing seawater maintained between 18 and 20°C in a room with a skylight and exposed only to natural illumination. Natural light intensities near the surface of the water were monitored continuously using a HOBO light data logger (Onset Computer Corporation, Pocasset, MA, USA). They peaked midday at approximately 70,000 lx. The spectrum of light in the aquarium room was also measured from 300 to 850 nm using an Ocean Optics USB4000 UV-visible spectrometer fitted with a 200 µm diameter UV-visible fiber. No light with wavelengths below 400 nm penetrated the skylight. In

The Journal of Experimental Biology (2014) doi:10.1242/jeb.107383

experiments designed to examine the effects of light on rhabdomeral LpUVOps1 levels, animals were exposed to full-spectrum sunlight by placing them in direct sunlight in an open, outdoor aquarium. The outdoor aquarium was supplied with natural, continuously flowing seawater at ambient temperature and a depth of approximately 18 cm above a white sandy bottom. The solar spectrum over the aquarium measured midday in June was calibrated to a NIST traceable standard (Ocean Optics LS-1-CAL). It was similar to those measured previously (Munz and McFarland, 1977, Loew and McFarland, 1990) with significant UV light down to 300 nm. Light levels immediately above the outdoor aquarium were also monitored with a HOBO light data logger; they peaked midday at approximately 250,000 lx. Animals exposed to direct sunlight were placed in the outdoor aquarium 30 min before sunrise. Eyes of some animals were fixed in the light 30 min after peak illumination during the day. Other animals were held in the outdoor aquarium from before sunrise until sunset, when they were brought into an indoor aquarium and kept in the dark until their eyes were fixed under dim red light 4 h after sunset.

Reagents

Unless otherwise specified, reagents were purchased from Fisher Scientific (Pittsburgh, PA, USA) or Sigma-Aldrich (St Louis, MO, USA).

Cloning a presumptive *L. polyphemus* UV opsin

Three nucleotide fragments with high homology to UV opsins from jumping spiders [*Hasarius adansoni* (HaRh3), AB251848; *Plexippus paykulli* (PpRh3), AB251851] (Koyanagi et al., 2008) were identified in 454 transcriptome analyses of cDNA libraries of VEs and the central nervous system (CNS). Two identical fragments, one from the VEs and the other from the CNS, encoded a sequence that aligned with amino acids 23–95 in HaRh3 (48% identical). Another fragment from the CNS encoded a sequence that aligned with amino acids 139–186 in HaRh3 (61% identical). PCR primers designed to amplify between the two transcriptome fragments (6387567-F1 and 6189070-R2; supplementary material Table S1) produced a predicted 500 bp amplicon from cDNA libraries of *L. polyphemus* VEs and CNS and from a cDNA library of *L. polyphemus* MEs (Smith et al., 1993). The 500 bp amplicon was extended with a rapid amplification of cDNA ends (RACE) strategy, using a VE cDNA library as template and 5′ and 3′ adaptor primers (supplementary material Table S1). The entire open reading frame of the opsin was amplified from the VE cDNA library using primers specific for sequences within the 5′ and 3′ untranslated regions. The resulting 1386 bp piece included both start and stop codons. Three separate full-length clones were sequenced in forward and reverse directions to obtain a consensus sequence. PCR and RACE reactions were performed using LATaq polymerase (Takara, Madison, WI, USA) and an Eppendorf Mastercycler (Hauppague, NY, USA).

Phylogenetic analysis

The predicted amino acid sequence of the opsin was aligned with other arthropod opsin sequences downloaded from GenBank (http://ncbi.nlm.nih.gov/Genbank/) and analyzed on the Phylogeny.fr platform (www.phylogeny.fr/version2_cgi/phylogeny.cgi) (Henze et al., 2012). The outgroups were two cephalopod opsins and mouse melanopsin. A graphical representation of the phylogenetic tree was obtained using TreeDyn v198.3 (Chevenet et al., 2006) and edited in CorelDRAW (Ottawa, ON, Canada). Accession numbers for sequences included in the tree are in supplementary material Table S2.

Tissue distribution of the opsin transcripts

Aliquots of LE and ME cDNA libraries (Smith et al., 1993) and an expressed sequence tag collection from VEs (Katti et al., 2010) were probed for the presumptive UV opsin transcript with PCR and primers 6387567 F1 and 6189070 R2.

In situ hybridization

Antisense and sense digoxigenin-labeled RNA probes were generated from the full-length coding region of the opsin using T3 or T7 RNA polymerases and a DIG RNA labeling protocol (Roche Applied Science, Penzberg, Germany).

VEs were dissected in *L. polyphemus* saline (Warren and Pierce, 1982), fixed for 2 h on ice in 4% paraformaldehyde (PFA) in phosphate buffered saline (PBS: 11.9 mmol l^{-1} phosphate buffer pH 7.2, 0.5 mol l^{-1} NaCl) and processed for *in situ* hybridization as whole mounts (Jezzini et al., 2005). The probe was visualized with Fab fragments of an anti-digoxigenin antibody, followed by the NBT/BCIP reaction (Roche Applied Science). LEs and MEs were dissected in *L. polyphemus* saline, fixed for 2 h on ice with 4% PFA in PBS containing 4.5% sucrose, dehydrated and rehydrated (Jezzini et al., 2005), then incubated overnight at 4°C in 0.1 mol l^{-1} phosphate buffer pH 7.2 (PB) containing 30% sucrose. Tissues were frozen in OCT 4583 Compound (Tissue-Tek, Sakura Finetek, Torrance, CA, USA) and sections were cut with a CM3050S Cryostat (Leica Microsystems, Mannheim, Germany). *In situ* hybridizations were performed as described above, and then processed according the TSA plus protocol (PerkinElmer, Waltham, MA, USA). Probes were visualized as fluorescein or cyanine 3 fluorescence using a confocal microscope (Leica SP5, Leica Microsystems).

Antibody production

cDNA encoding the C terminus of the presumptive UV opsin (L^{346}–G^{358}) (Fig. 2) was subcloned into pET28a (Novagen, EMD Chemicals, Gibbston, NJ, USA) at the HindIII and NdeI sites. After the sequence of the insert was confirmed, the pET 28a plasmid containing the insert was transformed into *Escherichia coli* (Rosetta: Novagen, EMD Chemicals), and the polypeptide was expressed using standard protocols. The expressed polypeptide was insoluble, so it was extracted in 6 mol l^{-1} urea, enriched by standard Ni^{+} chelation chromatography in urea (PrepEase His-Tagged Purification Midi Kit-High specificity, Affymetrix/USB, Santa Clara, CA, USA) and dialyzed overnight against PBS. A battery of hybridoma cell lines was prepared as described previously (Katti et al., 2010). Monoclonal antibody 57-62 (Isotype IgG2A, Kappa) was used in all experiments described in this study.

SDS-PAGE

Proteins were separated on NuPAGE 4-12% Bis-Tris Mini Gels (Novex, Life Technologies, Grand Island, NY, USA) using the manufacturer's protocol.

Membrane preparation, quantifying antigens, western blotting and immunostaining western blots

These protocols are detailed elsewhere (Battelle et al., 2001; Katti et al., 2010). Membranes were prepared from daytime, light-adapted eyes.

Tissue fixation and immunostaining

All tissues were fixed in ice-cold methanolic formaldehyde (Katti et al., 2010), except those VE preparations used to detect neurobiotin (see below). The time of day and lighting conditions at the time of fixation are indicated in the legends to the figures. In some experiments, VEs were dissected and desheathed in *L. polyphemus* saline (Warren and Pierce, 1982), then fixed and immunostained as whole mounts. Alternatively, VEs were fixed within a block of tissue that also included the brain and ventral cuticle. After the fixed tissue was rehydrated, VEs, including their EOs, were dissected in PB, cryoprotected in 30% sucrose in PB, frozen in OCT, sectioned and immunostained as described previously (Calman et al., 1991). For immunostaining whole mounts the immunostaining protocol was modified as follows. Tissues were permeabilized in 0.4% Triton X 100 for 2 h, primary antibody was applied overnight at 4°C and secondary antibody was applied for 2 h at room temperature. Between and after application of each antibody, tissues were rinsed three times for 30 min each time. Absorption controls were performed as described previously (Katti et al., 2010).

In addition to monoclonal antibody 57-62 described above, tissues were immunostained with a rabbit polyclonal antibody directed against LpOps1-2 (Battelle et al., 2001), mouse monoclonal antibody 4D10 directed against the N-terminal half of *L. polyphemus* arrestin (isotype IgG2B) (Battelle et al., 2000), mouse monoclonal antibody 2-449 directed against LpOps5 (isotype IgG1) (Katti et al., 2010) and a rabbit polyclonal antibody directed against $G_{q/11}\alpha$ (C-19, Santa Cruz Biotechnology, Santa Cruz, CA, USA) (Munger et al., 1996). Neurobiotin was detected with an anti-biotin antibody

(Vector Laboratories, Burlingame, CA, USA). AlexaFluor-labeled secondary antibodies were purchased from Life Technologies.

Imaging and quantifying immunoreactivity on sections

Images were collected using a Leica Sp5 confocal microscope. Images to be compared directly were collected during the same confocal session using identical settings. To quantify immunoreactivity at rhabdoms, average maximum immunoreactive intensities associated with rhabdoms were determined from maximum projections of stacks of confocal images using the line profile tool of the Leica SP5 software. Three measurements were made for each rhabdom to determine the average maximum intensity for that rhabdom (see supplementary material Fig. S3). Significance of differences in levels of rhabdomeral immunoreactivity was tested with the Student's *t*-test.

Electrophysiological recordings

VE nerves were dissected during the day (Clark et al., 1969) and then left in darkness overnight at 4°C in *L. polyphemus* organ culture medium (Kass et al., 1988; modified from Bayer and Barlow, 1978). Subsequent recordings were made in artificial seawater containing (in mmol l^{-1}): 435 NaCl, 10 KCl, 20 $MgCl_2$, 25 $MgSO_4$, 10 $CaCl_2$ and 10 HEPES at pH 7.2. To record electrical activity, cells were impaled with glass micropipettes pulled to a resistance of 30–100 MΩ when filled with 3 mol l^{-1} KCl.

Light from a 75 W Xenon arc source (Deltascan D101, PTI Inc., Birmingham, NJ, USA) was focused by a reflector onto the slit of a monochromator set to 5 nm bandwidth and refocused through a shutter onto a light guide (Ocean Optics P400-1-SR). The output of the light guide was positioned immediately above the surface of the artificial seawater surrounding the dissected VE nerve. The energy of light emitted from the light guide at each wavelength was measured using a spectrophotometer (Ocean Optics USB4000) and a photon-counting photomultiplier (Hamamatsu R928). Spectral sensitivity curves were corrected for relative differences in light output with wavelength.

Spectral sensitivity was determined as described previously (Nolte and Brown, 1969). At each wavelength, ND filters were inserted into the light path to generate responses within 5 mV of a criterion magnitude, set for each cell between 15 and 30 mV. When responses fell to either side of the criterion, the light intensity required to evoke the criterion response was estimated by interpolation. The reciprocal of the intensity at each wavelength producing the criterion response was defined as the spectral sensitivity. The peak of each spectral sensitivity curve was arbitrarily set to zero log units of attenuation. The accuracy of these measurements was limited for cells in which photon shot noise was comparable to the 5 mV range for determining the criterion, resulting in some uncertainty in determining spectral curve peaks.

To fill cells with neurobiotin, blunt thin-walled glass micropipettes were filled with 2% neurobiotin (Vector Laboratories) in 1 mol l^{-1} KCl, which was injected into the cells by rapid pressure injection (Corson and Fein, 1983). The locations of filled cells along each root were mapped. After all cells were filled, VE nerves were fixed in 4% PFA (Battelle et al., 2001) and immunostained as whole mounts as described above to detect neurobiotin and LpUVOps1. Immunostained cells were visualized with confocal microscopy.

Image preparation

Images were intensified in CorelDRAW X3 or Adobe Photoshop CS2 (Adobe Systems Inc., San Jose, CA, USA) and assembled in CorelDRAW X3.

Acknowledgements

We thank Jennifer Blythe for technical assistance, Dr Karen L. Carleton for measuring the spectrum of light over Whitney's indoor and outdoor aquaria, and Drs Abner B. Lall and W. Clay Smith for helpful comments on an earlier draft of the manuscript. A. Harrison was a participant in the Whitney Laboratory's NSF-Sponsored Research Experience for Undergraduates program.

Competing interests

The authors declare no competing financial interests.

Author contributions

B.-A.B. and R.P. were responsible for the study's conception and design. All authors contributed to the study's execution and interpretation of findings. B.-A.B., R.P. and K.E.K. were responsible for drafting and revising the manuscript.

Funding

This work was supported by the National Science Foundation [IOS1146175 and DBI 0648969 to B.-A.B.], the Core Facilities of the College of Computer, Mathematical, and Natural Sciences, University of Maryland, College Park and National Institutes of Health [EY021721], and Research to Prevent Blindness grants to the Department of Ophthalmology Core Facilities, University of Florida. Deposited in PMC for release after 12 months.

Supplementary material

Supplementary material available online at
http://jeb.biologists.org/lookup/suppl/doi:10.1242/jeb.107383/-/DC1

References

Battelle, B. A., Andrews, A. W., Kempler, K. E., Edwards, S. C. and Smith, W. C. (2000). Visual arrestin in *Limulus* is phosphorylated at multiple sites in the light and in the dark. *Vis. Neurosci.* **17**, 813-822.

Battelle, B. A., Dabdoub, A., Malone, M. A., Andrews, A. W., Cacciatore, C., Calman, B. G., Smith, W. C. and Payne, R. (2001). Immunocytochemical localization of opsin, visual arrestin, myosin III, and calmodulin in *Limulus* lateral eye retinular cells and ventral photoreceptors. *J. Comp. Neurol.* **435**, 211-225.

Battelle, B.-A., Kempler, K. E., Parker, A. K. and Gaddie, C. D. (2013). Opsin1-2, G(q)α and arrestin levels at *Limulus* rhabdoms are controlled by diurnal light and a circadian clock. *J. Exp. Biol.* **216**, 1837-1849.

Bayer, D. S. and Barlow, R. B., Jr (1978). *Limulus* ventral eye. Physiological properties of photoreceptor cells in an organ culture medium. *J. Gen. Physiol.* **72**, 539-563.

Behrens, M. E. and Fahy, J. L. (1981). Slow potentials in non-spiking optic-nerve fibers in the peripheral visual-system of *Limulus*. *J. Comp. Physiol.* **141**, 239-247.

Brown, J. E., Murray, J. R. and Smith, T. G. (1967). Photoelectric potential from photoreceptor cells ventral eye of *Limulus*. *Science* **158**, 665-666.

Britt, S. G., Feiler, R., Kirschfeld, K. and Zucker, C. S. (1993). Spectral tuning of rhodopsin and metarhodopsin *in vivo*. *Neuron* **11**, 29-39.

Calman, B. G. and Chamberlain, S. C. (1982). Distinct lobes of *Limulus* ventral photoreceptors. II. Structure and ultrastructure. *J. Gen. Physiol.* **80**, 839-862.

Calman, B. G., Lauerman, M. A., Andrews, A. W., Schmidt, M. and Battelle, B. A. (1991). Central projections of *Limulus* photoreceptor cells revealed by a photoreceptor-specific monoclonal antibody. *J. Comp. Neurol.* **313**, 553-562.

Chevenet, F., Brun, C., Bañuls, A.-L., Jacq, B. and Christen, R. (2006). TreeDyn: towards dynamic graphics and annotations for analyses of trees. *BMC Bioinformatics* **7**, 439-448.

Chou, W.-H., Hall, K. J., Wilson, D. B., Wideman, C. L., Townson, S. M., Chadwell, L. V. and Britt, S. G. (1996). Identification of a novel *Drosophila* opsin reveals specific patterning of the R7 and R8 photoreceptor cells. *Neuron* **17**, 1101-1115.

Clark, A. W., Millecchia, R. and Mauro, A. (1969). The ventral photoreceptor cells of *Limulus*. I. The microanatomy. *J. Gen. Physiol.* **54**, 289-309.

Corson, D. W. and Fein, A. (1983). Quantitative pressure injection of picoliter volumes into *Limulus* ventral photoreceptors. *Biophys. J.* **44**, 299-304.

Fahrenbach, W. H. (1975). The visual system of the horseshoe crab *Limulus polyphemus*. *Int. Rev. Cytol.* **41**, 285-349.

Fahrenbach, W. H. (1985). Anatomical circuitry of lateral inhibition in the eye of the horseshoe crab, *Limulus polyphemus*. *Proc. R. Soc. B* **225**, 219-249.

Fahrenbach, W. H. and Griffin, A. J. (1975). The morphology of the *Limulus* visual system. VI. Connectivity in the ocellus. *Cell Tissue Res.* **159**, 39-47.

Fliesler, S. J. (1993). *In vitro* biosynthetic studies with isolated vertebrate retinas. *Methods Neurosci.* **15**, 86-107.

Graham, C. H. and Hartline, H. K. (1935). The response of single visual sense cells to lights of different wavelengths. *J. Gen. Physiol.* **18**, 917-931.

Hartline, H. K., Wagner, H. G. and Ratliff, F. (1956). Inhibition in the eye of *Limulus*. *J. Gen. Physiol.* **39**, 651-673.

Harzsch, S., Vilpoux, K., Blackburn, D. C., Platchetzki, D., Brown, N. L., Melzer, R., Kempler, K. E. and Battelle, B. A. (2006). Evolution of arthropod visual systems: development of the eyes and central visual pathways in the horseshoe crab *Limulus polyphemus* Linnaeus, 1758 (Chelicerata, Xiphosura). *Dev. Dyn.* **235**, 2641-2655.

Henze, M. J., Dannenhauer, K., Kohler, M., Labhart, T. and Gesemann, M. (2012). Opsin evolution and expression in arthropod compound eyes and ocelli: insights from the cricket *Gryllus bimaculatus*. *BMC Evol. Biol.* **12**, 163-178.

Herman, K. G. (1991a). Two classes of *Limulus* ventral photoreceptors. *J. Comp. Neurol.* **303**, 1-10.

Herman, K. G. (1991b). Light-stimulated rhabdom turnover in *Limulus* ventral photoreceptors maintained *in vitro*. *J. Comp. Neurol.* **303**, 11-21.

Hu, X., Whaley, M. A., Stein, M. M., Mitchell, B. E. and O'Tousa, J. E. (2011). Coexpression of spectrally distinct rhodopsins in Aedes aegypti R7 photoreceptors. *PLoS ONE* **6**, e23121.

Hu, X., Leming, M. T., Metoxen, A. J., Whaley, M. A. and O'Tousa, J. E. (2012). Light-mediated control of rhodopsin movement in mosquito photoreceptors. *J. Neurosci.* **32**, 13661-13667.

Hu, X., Leming, M. T., Whaley, M. A. and O'Tousa, J. E. (2014). Rhodopsin coexpression in UV photoreceptors of *Aedes aegypti* and *Anopheles gambiae* mosquitoes. *J. Exp. Biol.* **217**, 1003-1008.
Jezzini, S. H., Bodnarova, M. and Moroz, L. L. (2005). Two-color in situ hybridization in the CNS of *Aplysia californica*. *J. Neurosci. Methods* **149**, 15-25.
Jones, C., Nolte, J. and Brown, J. E. (1971). The anatomy of the median ocellus of *Limulus*. *Z. Zellforsch. Mikrosk. Anat.* **118**, 297-309.
Kass, L., Pelletiler, J. L., Renninger, G. H. and Barlow, Jr., R. B. (1988) Efferent neurotransmission of circadian rhythms in *Limulus* lateral eye. II. Intracellular recordings *in vitro*. *J. Comp. Physiol. A* **164**, 95-105.
Katti, C., Kempler, K., Porter, M. L., Legg, A., Gonzalez, R., Garcia-Rivera, E., Dugger, D. and Battelle, B. A. (2010). Opsin co-expression in *Limulus* photoreceptors: differential regulation by light and a circadian clock. *J. Exp. Biol.* **213**, 2589-2601.
Knox, B. E., Salcedo, E., Mathiesz, K., Schaefer, J., Chou, W. H., Chadwell, L. V., Smith, W. C., Britt, S. G. and Barlow, R. B. (2003). Heterologous expression of *Limulus* rhodopsin. *J. Biol. Chem.* **278**, 40493-40502.
Koyanagi, M., Nagata, T., Katoh, K., Yamashita, S. and Tokunaga, F. (2008). Molecular evolution of arthropod color vision deduced from multiple opsin genes of jumping spiders. *J. Mol. Evol.* **66**, 130-137.
Lall, A. B. (1970). Spectral sensitivity of intracellular responses from visual cells in median ocellus of *Limulus polyphemus*. *Vision Res.* **10**, 905-909.
Lasansky, A. (1967). Cell junctions in ommatidia of *Limulus*. *J. Cell Biol.* **33**, 365-383.
Loew, E. R. and McFarland, W. N. (1990). The underwater visual environment. In *The Visual System of Fish* (ed. R. H. Douglas and M. B. A. Djamgoz), pp. 1-43. London: Chapman and Hall.
Munger, S. D., Schremser-Berlin, J. L., Brink, C. M. and Battelle, B. A. (1996). Molecular and immunological characterization of a Gq protein from ventral and lateral eye of the horseshoe crab *Limulus polyphemus*. *Invert. Neurosci.* **2**, 175-182.
Munz, F. W. and McFarland, W. N. (1977). Evolutionary adaptations of fishes to the photic environment. In *The Visual System in Vertebrates* (ed. F. Crescitelli), pp. 194-274. New York, NY: Springer-Verlag.
Murray, G. C. (1966). Intracellular absorption difference spectrum of *Limulus* extra-ocular photolabile pigment. *Science* **154**, 1182-1183.
Nolte, J. and Brown, J. E. (1969). The spectral sensitivities of single cells in the median ocellus of *Limulus*. *J. Gen. Physiol.* **54**, 636-649.
Nolte, J. and Brown, J. E. (1970). The spectral sensitivities of single receptor cells in the lateral, median, and ventral eyes of normal and white-eyed Limulus. *J. Gen. Physiol.* **55**, 787-801.
Nolte, J. and Brown, J. E. (1972). Electrophysiological properties of cells in the median ocellus of *Limulus*. *J. Gen. Physiol.* **59**, 167-185.
Ogawa, Y., Awata, H., Wakakuwa, M., Kinoshita, M., Stavenga, D. G. and Arikawa, K. (2012). Coexpression of three middle wavelength-absorbing visual pigments in sexually dimorphic photoreceptors of the butterfly *Colias erate*. *J. Comp. Physiol. A* **198**, 857-867.
Palczewski, K., Kumasaka, T., Hori, T., Behnke, C. A., Motoshima, H., Fox, B. A., Le Trong, I., Teller, D. C., Okada, T., Stenkamp, R. E. et al. (2000). Crystal structure of rhodopsin: A G protein-coupled receptor. *Science* **289**, 739-745.
Patten. W. (1894). On the morphology and physiology of the brain and sense organs of *Limulus*. *Q. J. Microsc. Sci.* **3,** 1-96.
Porter, M. L., Cronin, T. W., McClellan, D. A. and Crandall, K. A. (2007). Molecular characterization of crustacean visual pigments and the evolution of pancrustacean opsins. *Mol. Biol. Evol.* **24**, 253-268.
Porter, M. L., Speiser, D. I., Zaharoff, A. K., Caldwell, R. L., Cronin, T. W. and Oakley, T. H. (2013). The evolution of complexity in the visual systems of stomatopods: insights from transcriptomics. *Integr. Comp. Biol.* **53**, 39-49.
Regier, J. C., Shultz, J. W., Zwick, A., Hussey, A., Ball, B., Wetzer, R., Martin, J. W. and Cunningham, C. W. (2010). Arthropod relationships revealed by phylogenomic analysis of nuclear protein-coding sequences. *Nature* **463**, 1079-1083.
Salcedo, E., Zheng, L., Phistry, M., Bagg, E. E. and Britt, S. G. (2003). Molecular basis for ultraviolet vision in invertebrates. *J. Neurosci.* **23**, 10873-10878.
Smith, T. G. and Baumann, F. (1969). The functional organization within the ommatidium of the lateral eye of *Limulus*. *Prog. Brain Res.* **31**, 313-349.
Smith, W. C., Price, D. A., Greenberg, R. M. and Battelle, B. A. (1993). Opsins from the lateral eyes and ocelli of the horseshoe crab, *Limulus polyphemus*. *Proc. Natl. Acad. Sci. USA* **90**, 6150-6154.
Stavenga, D. G. (2010). On visual pigment templates and the spectral shape of invertebrate rhodopsins and metarhodopsins. *J. Comp. Physiol. A* **196**, 869-878.
Stavenga, D. G., Smits, R. P. and Hoenders, B. J. (1993). Simple exponential functions describing the absorbance bands of visual pigment spectra. *Vision Res.* **33**, 1011-1017.
Wald, G. and Hubbard, R. (1950). The synthesis of rhodopsin from vitamin A_1. *Proc. Natl. Acad. Sci. USA* **6**, 92-102.
Warren, M. K. and Pierce, S. K. (1982). Two cell-volume regulatory systems in the *Limulus* myocardium – an interaction of ions and quaternary ammonium-compounds. *Biol. Bull.* **163**, 504-516.
Wasserman, G. S. (1969). *Limulus* receptor action spectra. *Vision Research* **9**, 611-620.
Waterman, T. H. and Wiersma, C. A. G. (1954). The functional relation between retinal cells and optic nerve in *Limulus*. *J. Exp. Zool.* **126**, 59-85.
Yokoyama, S. (2000). Molecular evolution of vertebrate visual pigments. *Prog. Retin. Eye Res.* **19**, 385-419.